Biomed Microdevices (2014) 16:79–90
DOI 10.1007/s10544-013-9807-3

Single-cell analysis of embryoid body heterogeneity using microfluidic trapping array

Jenna L. Wilson · Shalu Suri · Ankur Singh · Catherine A. Rivet · Hang Lu · Todd C. McDevitt

Published online: 2 October 2013

Abstract The differentiation of pluripotent stem cells as embryoid bodies (EBs) remains a common method for inducing differentiation toward many lineages. However, differentiation via EBs typically yields a significant amount of heterogeneity in the cell population, as most cells differentiate simultaneously toward different lineages, while others remain undifferentiated. Moreover, physical parameters, such as the size of EBs, can modulate the heterogeneity of differentiated phenotypes due to the establishment of nutrient and oxygen gradients. One of the challenges in examining the cellular composition of EBs is the lack of analytical methods that are capable of determining the phenotype of all of the individual cells that comprise a single EB. Therefore, the objective of this work was to examine the ability of a microfluidic cell trapping array to analyze the heterogeneity of cells comprising EBs during the course of early differentiation. The heterogeneity of single cell phenotype on the basis of protein expression of the pluripotent transcription factor OCT-4 was examined for populations of EBs and single EBs of different sizes at distinct stages of differentiation. Results from the cell trap device were compared with flow cytometry and whole mount immunostaining. Additionally, single cells from dissociated pooled EBs or individual EBs were examined separately to discern potential differences in the value or variance of expression between the different methods of analysis. Overall, the analytical method described represents a novel approach for evaluating how heterogeneity is manifested in EB cultures and may be used in the future to assess the kinetics and patterns of differentiation in addition to the loss of pluripotency.

Keywords Stem cells · Embryoid bodies · Heterogeneity · Microfluidics

Jenna L. Wilson and Shalu Suri contributed equally to this work

J. L. Wilson · C. A. Rivet · T. C. McDevitt (✉)
The Wallace H. Coulter Department of Biomedical Engineering, Georgia Institute of Technology and Emory University, 313 Ferst Drive, Suite 2102, Atlanta, GA 30332-0532, USA
e-mail: todd.mcdevitt@bme.gatech.edu

S. Suri · H. Lu
School of Chemical & Biomolecular Engineering, Georgia Institute of Technology, Atlanta, GA, USA

A. Singh
The George W. Woodruff School of Mechanical Engineering, Georgia Institute of Technology, Atlanta, GA, USA

H. Lu · T. C. McDevitt
The Parker H. Petit Institute for Bioengineering and Bioscience, Georgia Institute of Technology, Atlanta, GA, USA

1 Introduction

Pluripotent embryonic stem cells (ESCs) have many potential applications as a cell source for regenerative medicine and as a vehicle to attain new insights into embryonic development. Though ESCs are clonal and therefore are often assumed to exist as a homogenous cell population, there are subtle discrepancies in cell phenotype even in the undifferentiated state prior to the induction of differentiation (Hayashi et al. 2008; Toyooka et al. 2008). It has been suggested that undifferentiated stem cells exist as a heterogeneous population so they can be simultaneously influenced to differentiate while also maintaining their ability for self-renewal (Graf and Stadtfeld 2008). Heterogeneity may result from the ability of a single cell type to interconvert stochastically between different pluripotent states, as it has been observed that ESCs can occupy a continuum of cell states, each with their own distinct phenotypic characteristics (Hough et al. 2009). Examples of *in vivo* heterogeneity of pluripotent cells, such as the "salt-and-pepper" expression of transcription factors in the inner cell mass (Chazaud et al. 2006), imply that such diversity is not

simply a product of *in vitro* culture; in fact, the diversity may confer an innate response to environmental or physiological stress (Enver et al. 2009) via cells existing in a bivalent state in which they are primed for differentiation while retaining self-renewal capacity (Silva and Smith 2008). In addition to heterogeneity of the pluripotent state of ESC populations, often some level of spontaneous differentiation exists within the undifferentiated population of cells (Enver et al. 2005). Attempts to direct the differentiation of an initially heterogeneous population of stem cells is likely to compromise the overall yield and efficiency, as cells in different states may respond differentially to the same stimuli. Thus, in order to efficiently proceed with stem cell applications and directed differentiation methods, it is necessary to understand and account for the presence of multiple cell states within a population of stem cells.

Embryonic stem cells are often differentiated as three-dimensional multicellular aggregates referred to as "embryoid bodies" (EBs) due to their ability to spontaneous yield derivatives of the three germ lineages simultaneously (Doetschman et al. 1985). EB differentiation is commonly used to model morphogenesis in addition to differentiation since analogous structures and patterns are observed within EBs that mimic the morphogenic events of early embryonic development (Antonica et al. 2012; Eiraku et al. 2011; Keller 2005; Leahy et al. 1999; Sajini et al. 2012; Suga et al. 2011). Significant research has been conducted to examine the ability of different biochemical and environmental factors to direct EB differentiation (Bratt-Leal et al. 2009; Kurosawa 2007), and EB formation remains a critical step in many differentiation protocols (Doetschman et al. 1985; Esner et al. 2002; Kattman et al. 2006; Ng et al. 2005; Risau et al. 1988; Wichterle et al. 2002; Xu et al. 2002). Differentiation of cells as three-dimensional multicellular aggregates inherently adds the complication of spatial gradients that can differentially impact cell phenotypes between the center and exterior of EBs (Van Winkle et al. 2012). Consequently, the size of EBs used has been found to impact the differentiation propensity (Choi et al. 2010; Hong et al. 2010; Messana et al. 2008; Niebruegge et al. 2009; Valamehr et al. 2008); for example, larger EBs tend to have a greater tendency toward cardiac differentiation than smaller EBs (Bauwens et al. 2008; Hwang et al. 2009; Mohr et al. 2010) . However, it is difficult to directly compare studies since EB formation methods and size ranges differ from study to study, thus definitive correlations between size and differentiated phenotypes have been mixed. Furthermore, aggregate size alone does not account for all the variance in EB phenotype, as heterogeneity between EBs of the same size is often observed (Bratt-Leal et al. 2009), even when all other parameters are seemingly taken into account.

One of the challenges of investigating the cellular composition of EBs is the deficiency of current analytical methods to determine the phenotype of all of the individual cells that comprise a single aggregate. Examining phenotypic properties on a single cell level provides more information than population averaging-based methods, as one can discern whether a small subpopulation is solely responsible for the change in expression or if all cells in the population are undergoing similar changes (Schroeder 2011). Previous research has demonstrated that ESC gene expression results differ greatly when examined at a single cell, rather than a population, level (Zhong et al. 2008), further motivating the development of high throughput methods for investigating single stem cell fate. Existing methods, such as flow cytometry, provide a high-throughput means to analyze phenotypic characteristics of a cell population, but typically require cell quantities ($10^{5\text{-}6}$) that are much greater than the number of cells comprising a single multicellular aggregate ($10^{3\text{-}4}$). Confocal microscopy, another common analytical method, is a low-throughput process that has a limited capacity to image three-dimensional tissues (Buschke et al. 2010; Chung et al. 2013; Jung et al. 2012). Due to the high cell density of EBs (Bratt-Leal et al. 2009), which do not exhibit a large degree of extracellular matrix at early stages of differentiation (Nair et al. 2012), imaging greater than 50 μm into an EB has been challenging due to optical limitations.

Analytical techniques that enable increased understanding of when and where heterogeneity is occurring in a cell population could lead to better assessments of directed differentiation techniques. Therefore, the objective of this study was to develop an approach to analyze the individual phenotypes of cells not only from populations of EBs, but from single EBs as well. To achieve this, a microfluidic cell trap device originally designed to examine calcium dynamics in Jurkat cells (Chung et al. 2011) was adapted and validated to examine expression of the pluripotent transcription factor OCT-4 in single cells from EBs of different sizes (defined by the initial number of cells per aggregate) and at different stages of differentiation. Additionally, single cells from dissociated pooled EBs or individual EBs were examined separately to discern potential differences in the value or variance of expression between the different methods of analysis. The results of this study indicate that examining single cell phenotype using a microfluidic approach can provide previously unidentified information about heterogeneity of EBs and may act as a complementary analysis method that provides more specific information regarding single stem cell fate(s) within complex multicellular aggregates.

2 Methods

2.1 Microfluidic device fabrication

Polydimethylsiloxane (PDMS) devices were fabricated via soft lithography rapid prototyping and replica molding,

followed by plasma-bonding onto glass slides (Chung et al. 2011). Briefly, negative molds were fabricated on silicon wafers using photoresist (SU8-2010, 14–16 μm, and SU8-2002, 1.5–3 μm thickness) (Microchem) and treated with tridecafluoro-1,1,2,2-tetrahydrooctyl-1-trichlorosilane vapor (United Chemical Technologies, Bristol, PA). PDMS with base polymer to crosslinker ratio of 10:1 was molded onto wafers and cured at 70 °C for 2 h. Individual devices were cut, access holes were punched and devices were bonded in an air plasma. Devices were stored at room temperature until further use.

2.2 Embryonic stem cell culture

Murine ESCs (D3 cell line) were cultured on tissue culture-treated polystyrene dishes (Corning Inc., Corning, NY) adsorbed with 0.1 % gelatin (Millipore, EmbryoMax). Undifferentiated ESC culture media consisted of Dulbecco's modified Eagle's medium (DMEM) (Mediatech) supplemented with 15 % fetal bovine serum (Hyclone, Logan, UT), 100 U/mL penicillin, 100 μg/mL streptomycin, and 0.25 μg/mL amphotericin (Mediatech, Herndon, VA), 2 mM L-glutamine (Mediatech), 1× MEM non-essential amino acid solution (Mediatech), 0.1 mM 2- mercaptoethanol (Fisher Scientific, Fairlawn, NJ), and 10^3 U/mL of leukemia inhibitory factor (LIF) (ESGRO, Chemicon, Temecula, CA). Cultures were replenished with fresh media every other day and passaged at approximately 70 % confluence.

2.3 Embryoid body (EB) formation and culture

A single cell suspension of undifferentiated ESCs was obtained through dissociation of monolayer cultures with 0.05 % trypsin-EDTA (Mediatech). Aggregation of ESCs was achieved by centrifugation (200 rcf) of ESCs into 400 μm diameter polydimethylsiloxane (PDMS) micro-wells (Aggrewell™, Stem Cell Technologies, Vancouver, Canada), as previously reported (Kinney et al. 2012; Ungrin et al. 2008). The cell seeding density was varied to achieve approximately 250 or 1,000 cells per individual well. The ESCs were incubated in the wells for approximately 20 h in undifferentiated ESC culture media without LIF to allow for EB formation. The resulting EB population was transferred to suspension culture (approximately 1500 EBs in 10 mL of undifferentiated ESC culture media without LIF) in sterile 100× 15 mm bacteriological grade polystyrene Petri dishes (BD, Franklin Lakes, NJ) and maintained on rotary orbital shakers (Carpenedo et al. 2007) at a frequency of approximately 65 rpm. A 90 % media exchange was performed every other day following gravity-induced sedimentation of the EBs in 15 mL conical tubes. Suspension cultures were maintained for up to 10 days of differentiation.

2.4 Cell loading into microfluidic devices

At days 5 and 10 of differentiation, EBs were collected and dissociated into a single cell suspension by incubation in 0.25 % trypsin-EDTA and trituration every 5 min for 20 min. After 10 days of differentiation, individual EBs were manually removed from the plate, imaged, and similarly dissociated using 0.25 % trypsin. The resulting cell suspensions were centrifuged (200 rcf, 5 min) and resuspended in culture media supplemented with 3 mM EGTA for a 30 min incubation (37 °C) to inhibit intercellular adhesion and reduce clogging in the microfluidic device. A LIVE/DEAD cell assay (Invitrogen) was performed to evaluate cell viability post-loading. Prior to cell loading, the devices were perfused with a 2 % solution of bovine serum albumin (Millipore). Single cells were loaded into the devices by pipetting the cell suspension into an inlet made with a 19-gauge needle. The cells were loaded into the device by gravity-driven flow. Once loaded, the device was perfused with a 4 % paraformaldehyde solution (Alfa Aesar) for 10 min to fix cells. Cells were also collected at day 0 (prior to EB formation) and similarly loaded into the devices. Cell-laden devices were stored with PBS at 4 °C until immunofluorescent staining was performed for parallel samples at the same time.

2.5 On-chip immunofluorescent staining

Immunofluorescent staining was performed in the devices by attaching a pipette tip containing the solution into the inlet and attaching 2.5 ft of polyethylene tubing (PE3, Scientific Commodities) to the outlet to induce gravity-driven flow. The cells were permeabilized with 0.05 % Triton X and 2 % donkey serum in PBS for 45 min at room temperature prior to overnight incubation at 4 °C with the primary antibody against OCT-4 (Santa Cruz Biotechnology sc-8628; 1:100 in 2 % donkey serum in PBS). The devices were perfused with PBS for 15 min to wash the cells prior to 1 h incubation with the secondary antibody solution (1:200 AlexaFluor®488 donkey anti-goat in 2 % donkey serum in PBS). The devices were perfused with PBS for 15 min to wash the cells prior to 10 min incubation with blue whole cell stain (HCS CellMask™, Invitrogen). A final 15 min perfusion with PBS was performed prior to imaging.

2.6 Cell trap imaging and image analysis

The devices were imaged using a Nikon TE 2000 inverted microscope equipped with a SPOT Flex camera (Diagnostic Instruments). Each chamber in the device was imaged on three channels (phase, Hoechst, and FITC). Image analysis was performed using ImageJ software (http://rsbweb.nih.gov/ij/). A threshold was applied to the whole cell stain image (blue

channel) to determine the cell area. Subsequently, the fluorescent intensity of OCT-4 staining (green channel) was determined for individual cells and normalized to the cell area. Area and intensity values were exported to Microsoft Excel for further analysis.

2.7 Flow cytometry

EBs were collected and dissociated into a single cell suspension through incubation in 0.25 % trypsin-EDTA and trituration every 5 min for 30 min. Cells were also collected at day 0 prior to EB formation. The cell suspension was centrifuged (200 rcf, 5 min) and resuspended in culture media supplemented with 3 mM EGTA for 30 min incubation (37 °C), as was performed prior to loading in the microfluidic devices. Cells were fixed in 4 % paraformaldehyde, washed 3× with PBS, and stored at 4 °C until staining was performed. Cells were permeabilized in 0.05 % Triton X-100 in blocking buffer (1 mg/ml BSA and 0.1 % Tween20 in PBS) for 30 min, then washed in blocking buffer for 15 min. Cells were incubated at room temperature with the primary antibody against OCT-4 (Santa Cruz Biotechnology sc-101462; 1 μg/million cells) for 1 h. Cells were washed with blocking buffer, then incubated with the secondary antibody (AlexaFluor®488 donkey anti-goat at 1 μg/million cells) for 30 min at room temperature. The cells were resuspended in 300 μL blocking buffer, filtered through the 35 μm cell-strainer cap of a 5 mL polystyrene round-bottom tube (BD Biosciences, San Jose, CA), and analyzed with an Accuri C6 flow cytometer for a minimum of 10,000 events. Normal goat IgG was used in place of primary antibody incubation as an isotype control, with positive gates set above 2 % of the IgG isotype control population. Analysis was performed using FlowJo software (Tree Star, Inc., Ashland, OR).

2.8 Whole mount staining and imaging

EBs were washed in PBS, fixed for 30 min in 4 % paraformaldehyde, and washed 3× with PBS. EBs were stored in PBS at 4 °C until staining was performed. EBs were permeabilized for 30 min in 1.5 % Triton X-100, re-fixed in 4 % paraformaldehyde for 15 min, and blocked in wash buffer (2 % donkey serum, 0.1 % Tween-20 in PBS) for 3 h. Samples were incubated in OCT-4 primary antibody (Santa Cruz Biotechnology sc-8628; 1:100) overnight at 4 °C, rinsed with wash buffer (3 times, 15 min), and incubated with the secondary antibody solution (1:200 AlexaFluor®488 donkey anti-goat in wash buffer) and Hoechst (1:100) for 4 h at 4 °C. To image, samples were re-suspended in a low volume of wash buffer and imaged with a Zeiss LSM 700-405 confocal microscope (Carl Zeiss Inc.).

2.9 Statistics

All population-based experiments were performed with triplicate samples from independent conditions ($n=3$). The data is represented as the mean of the independent replicates, and the error bars represent the standard error of the mean. Before performing statistical analysis, data were normalized using a Box–Cox power transformation to equalize variance. A two-way ANOVA was calculated between the analysis method (cell trap and flow cytometry) and experimental groups, with post hoc Tukey analysis to determine significant differences ($p<0.05$) between the different analysis methods and experimental groups. A one-way ANOVA was calculated between the individual groups (population and single EB), with a post hoc Tukey analysis to determine significant differences ($p<0.05$) between the groups.

3 Results

3.1 Embryonic stem cell (ESC) on-chip analysis

To assess heterogeneity in the cell populations comprising embryoid bodies (EBs), murine embryonic stem cells were aggregated within PDMS microwells at two different seeding densities to form distinct EB sizes, transferred to suspension culture, and allowed to differentiate for up to 10 days (Fig. 1). After 5 days of differentiation, EBs of each size were dissociated into single cell suspensions, and the population from each plate was divided for cell trap and flow cytometry analysis. Intact EBs were also collected for whole mount immunostaining analysis. The single cell suspensions designated for cell trap analysis were loaded into the microfluidic device using gravity-driven flow as previously described (Chung et al. 2011). Populations of EBs were similarly processed after 10 days of differentiation, and single EBs were individually removed manually from the cultures, imaged, and dissociated prior to loading into cell trap devices.

Prior to EB formation, the ESC population used to form the EBs (Fig. 2a) was dissociated into single cells and loaded into cell trap devices or reserved for flow cytometric analysis. After 5 days of EB differentiation, differences in diameter were visually observed between the EBs initially seeded at a ratio of 250 cells per EB (Fig. 2b) and the EBs seeded at 1,000 cells per EB (Fig. 2c). By day 10 of differentiation (Fig. 2d, e), the presence of distinct EB sizes was no longer prevalent, though minor variability in size was observed in both cultures. Single cells derived from the different populations exhibited efficient cell loading into the device (Fig. 2f-o), with a low incidence of both empty traps and multiple cells per trap (<10 %). The cells were stained on-chip using a whole cell stain (blue), with the intensity remaining consistent throughout all groups (Fig. 2f-j). On-chip immunofluorescent staining

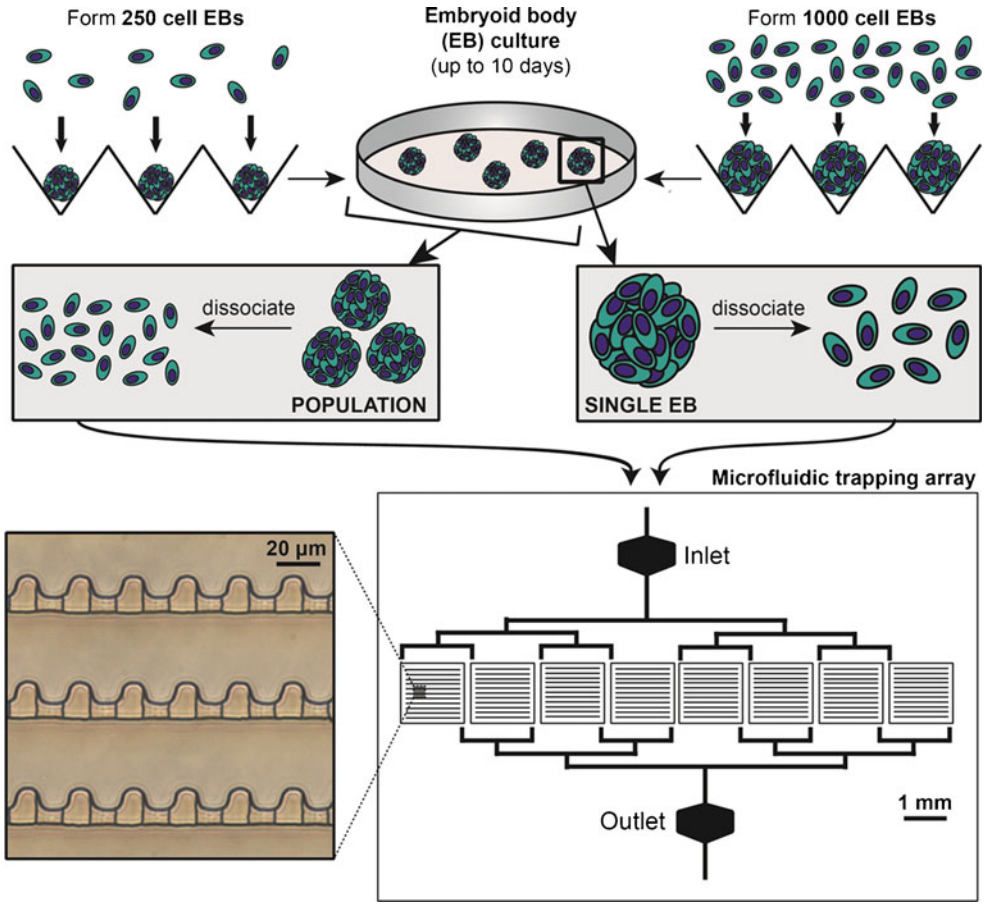

Fig. 1 Overview of experimental approach. Embryoid bodies (EBs) of 250 or 1,000 cells were formed via forced centrifugation in PDMS microwells and cultured for up to 10 days of differentiation. After 5 or 10 days of suspension culture, single cells were obtained from either from a dissociated population of EBs (~1,500 total) or from hand-picked individual aggregates, and loaded into the microfluidic cell trapping array for immunostaining and image analysis

for the pluripotent transcription factor OCT-4 was performed just prior to whole cell staining. The undifferentiated ESC population used for EB formation exhibited high intensity staining for OCT-4 at day 0 (Fig. 2k), and the intensity was reduced as the cells differentiated as EBs (Fig. 2l-o). After 5 days of differentiation, fewer cells expressed OCT-4 with an intensity as great as those observed with cells on day 0 (Fig. 2l, m) and majority of the cells had a faint antibody signal. At day 10 of differentiation, the cells from the 250 cell EBs appeared to have a relatively uniform additional attenuation of staining intensity (Fig. 2n). In comparison, qualitative analysis of the cells from the 1,000 cell EBs indicated that a sub-set of the population of cells retained high levels of OCT-4 expression, while most cells exhibited low to no expression of OCT-4 (Fig. 2o).

3.2 Examining populations of embryoid bodies (EBs) with cell traps and flow cytometry

In order to validate the cell trap analytical method, flow cytometry analysis was performed on cells dissociated from a population of EBs. Overall, both forms of analysis detected a similar decrease in OCT-4 expression (Fig. 3) as the cells differentiated. Based upon cell trap analysis, the 250 cell EB population exhibited an average intensity of 38 %±3 % and 16 %±3 % at days 5 and 10, respectively and relative to the day 0 ESCs. In comparison, analysis of the 1,000 cell EB population in the cell trap device displayed 44 %±22 % and 42 %±17 % of the day 0 intensity at days 5 and 10, respectively. The minor disparities between the cell trap and flow cytometry methods were not statistically significant ($p = 1.000$, 0.561, 0.198, 0.974).

A benefit of single cell analysis methods is the ability to examine the variance and heterogeneity of a cell population in addition to calculating simply population average information. Therefore, the OCT-4 intensity values were plotted as histograms in order to examine the variance of OCT-4 expression in the different groups. In general, OCT-4 expression was broadly expressed in the starting ESC population at day 0 (Fig. 4a, d), though several peaks were observed at higher intensities (10–20 units). While most devices exhibited a similar trend, some had a peak at a slightly lower intensity value that was not observed in the corresponding flow cytometry histogram (Fig. 4a inset). After 5 days of differentiation, there was little variability observed in the 250 cell EB population samples (Fig. 4b), whereas the 1,000 cell EBs appeared to have more variability between different populations at day 5 (Fig. 4e). After 10 days of differentiation, the variability of OCT-4 expression in the 250 cell EBs remained low (Fig. 4c),

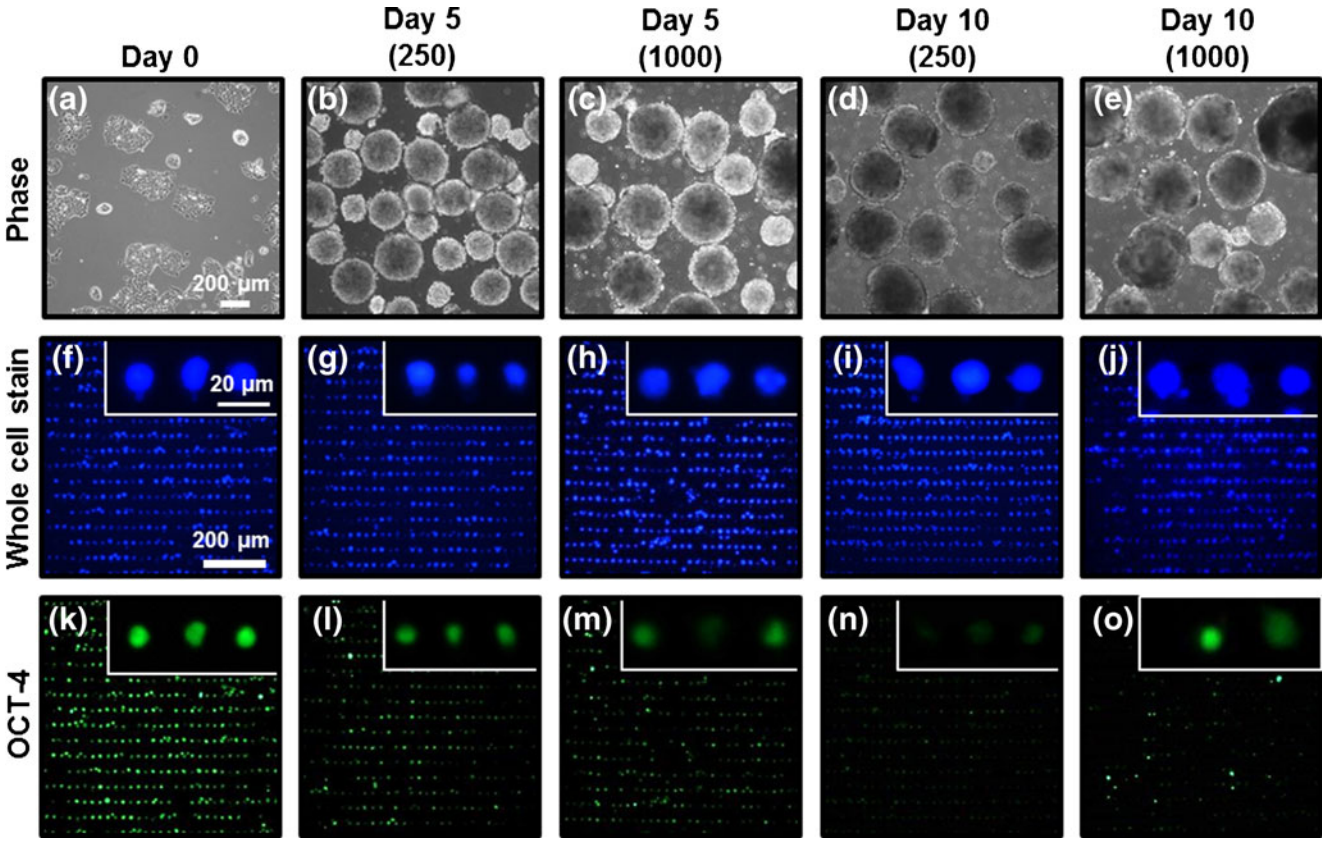

Fig. 2 Image time course and representative cell trap chamber images. Undifferentiated ESCs (**a**) were aggregated to form EBs comprised initially of 250 cells (**b**, **d**) or 1,000 cells (**c**, **e**). The dissociated EBs were loaded into the cell traps at days 5 and 10 of differentiation and stained with HCS CellMask™ (**f-j**) and an antibody against the pluripotent transcription factor OCT-4 (**k-o**). The initial undifferentiated ESC population exhibited bright staining for OCT-4 at day 0 (**k**), but the intensity decreased as expected as the cells differentiated as EBs (**l-o**)

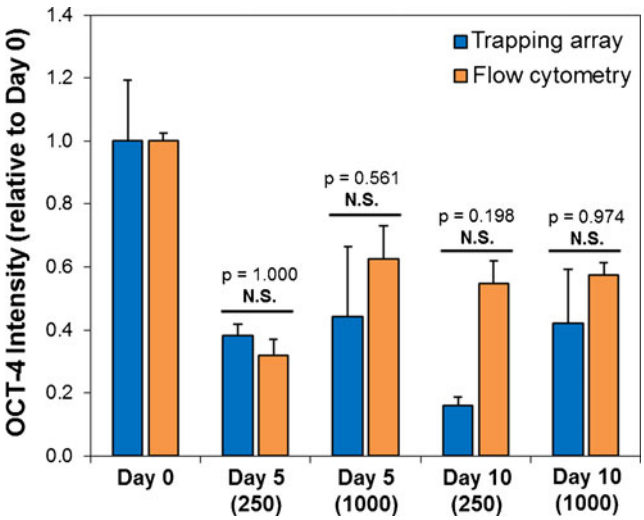

Fig. 3 Comparison of microfluidic trapping array and flow cytometry mean fluorescent intensities. The mean fluorescent intensities were calculated by averaging the intensity of individual cells within the cell trap devices or from the mean intensity values obtained by flow cytomery with a 533/30 nm filter and positive gates set at 2 % of the IgG isotype control population. No statistically significant differences were found between the two analytical methods ($p < 0.05$) at any of the time points examined

with decreased OCT-4 expression reflected by the narrowed peak of the intensity value and leftward shift. In the 1,000 cell EBs at day 10 (Fig. 4f), the expression pattern was similar to that at day 5, with more cells exhibiting greater OCT-4 intensity compared to the 250 cell EBs. In general, the shapes of the histograms of the cell trap analysis were in agreement with the flow cytometry results (Fig. 4 insets). For example, the flow cytometry histograms for the 1,000 cell EBs at day 5 (Fig. 4e) also exhibited a higher degree of variability amongst individual experimental replicates.

3.3 Comparing expression and heterogeneity of single EBs to population values

The microfluidic cell trap device has the unique ability to efficiently and rapidly trap cells from a single EB, thus enabling the analysis of inter-EB variability that could be masked in more common population-based methods. Confocal microscopy techniques allow for examination of the cellularity of single EBs; however, imaging is a low-throughput method that is limited by the lack of complete optical sectioning through densely packed multicellular

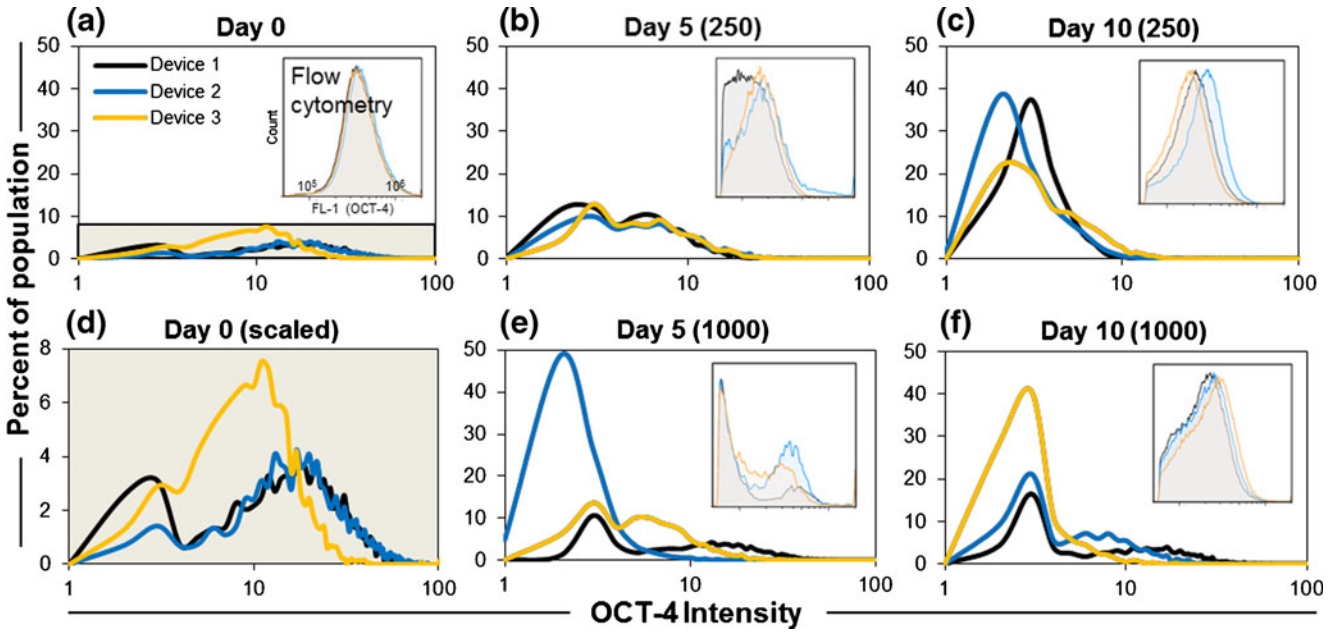

Fig. 4 Histogram analysis of OCT-4 heterogeneity. The percentage of the population with a given OCT-4 intensity (log scale) was plotted to display the value of the peak intensity as well as the width of the peak for the day 0 undifferentiated starting population (**a**, **d**), the 250 cell (**b**) and 1,000 cell (**e**) EBs at day 5 of differentiation, and the 250 cell (**c**) and 1,000 cell (**f**) EBs at day 10 of differentiation. The histogram outputs of the corresponding flow cytometry analysis (cell count vs. OCT-4 intensity) are displayed as insets

tissues (Buschke et al. 2010), restricting the information obtained for all the cells in a tissue or EB. For comparison with the single EB results from the cell trap, immunostaining for OCT-4 was performed on intact 250 cell and 1,000 cell EBs at days 5 and 10 differentiation, followed by confocal imaging in which optical sections were acquired (depth of 30 μm presented in Fig. 5). Decreasing expression of OCT-4 was observed in both sizes between days 5 and 10 of differentiation. After 5 days of differentiation, the 250 cell EBs (Fig. 5a) generally had similar OCT-4 expression, indicating low inter-EB variability, whereas increased variation was observed between EBs in the 1,000 cell EBs at day 5 (Fig. 5c). After 10 days of differentiation, spatially-constrained "pockets" of high and low OCT-4 expression were observed in both groups, though cells highly expressing OCT-4 appeared more frequently in the 1,000 cell EBs (Fig. 5d) than in the 250 cell EBs (Fig. 5b). These results clearly indicate an increased variability of OCT-4 expression within single EBs in comparison with the more uniform expression of OCT-4 by individual cells at day 5.

The differences in the intensity and spatial variance of OCT-4 expression within EBs of different sizes over time prompted further investigation into the single cell OCT-4 expression between individual EBs as compared to a population of EBs. Thus, single EBs were manually removed and dissociated individually prior to their loading into the cell trap devices, with approximately 45 % of the individual cells from a single EB successfully captured within a device. The reduced capture efficiency could be primarily attributed to the difficulty of dissociating a single EB and the subsequent transfer steps where many cells were lost. The ability to capture many cells from a single EB indicates the power of cell-trap devices despite the difficulty of working with such low cell populations.

The mean OCT-4 intensity values were compared for cells from populations and single EBs at day 10 of differentiation within the cell trap devices. Representative analyses of single EBs are presented in Fig. 6b (250 cells/EB) and 6c (1,000 cells/EB). In general, the single EBs exhibited lower OCT-4 expression levels than the population-averaged value (Fig. 6a), though this difference was not significant ($p=0.939$ for 250 cell EBs; $p=0.137$ for 1,000 cell EBs). A decrease ($p<0.05$) in OCT-4 expression relative to the day 0 ESC starting population was observed for three of the four experimental groups at day 10 of differentiation (250 cell EB population, averaged 250 cell single EBs, and averaged 1,000 cell single EBs), indicating that most experimental conditions had significantly decreased pluripotent transcription factor expression by day 10 of EB culture. The 1,000 cell EBs assessed at the population level did not exhibit a significant decrease in expression, which may indicate that the cells within the larger EBs may exhibit slower differentiation kinetics than the 250 cell EBs.

In an attempt to elucidate whether inter-EB or intra-EB heterogeneity was dominant in the different sizes, the values for each cell analyzed at day 10 of differentiation were arrayed with regard to intensity and cell size/area. Although the flow cytometry scatter plots for the population samples were

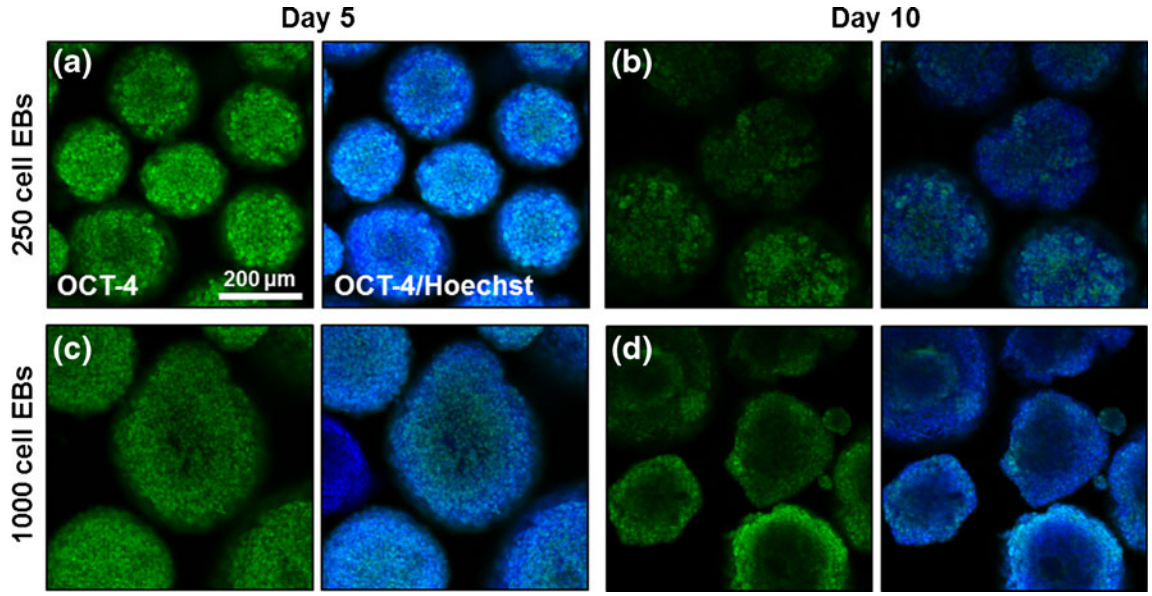

Fig. 5 Whole mount immunostaining for OCT-4 in intact EBs. EBs were collected at the same time points for which single cell expression was analyzed and stained for OCT-4 expression. Images represent optical sections at a 30 μm depth into the EB. The merged images (*right panels*) signify OCT-4 staining in addition to nuclear counterstaining with Hoechst. Relatively strong expression of OCT-4 was observed in both groups at day 5 (**a**, **c**). After 10 days of differentiation, OCT-4 expression decreased in both groups, though it appeared cells with high expression appear more frequently higher in the 1,000 cell EBs (**d**) than in the 250 cell EBs (**b**)

similar for the two EB sizes (Fig. 7a, d), the cell trap population scatter plots demonstrated that the 1,000 cell EB population (Fig. 7e) appeared more heterogeneous than the 250 cell EB population (Fig. 7b). The scatter plot for the 250 cell single EBs (Fig. 7c) had a similar appearance to the corresponding population scatter plot (Fig. 7b), suggesting that the heterogeneity of phenotypes within individual EBs was more prevalent than the overall heterogeneity between EBs of this size. In contrast, the 1,000 cell single EB data exhibited less heterogeneity than the EB population analysis (Fig. 7f), which indicates that inter-EB heterogeneity was more prevalent for larger EBs of this size.

4 Discussion

The differentiation of pluripotent stem cells as embryoid bodies (EBs) remains a common method for inducing differentiation

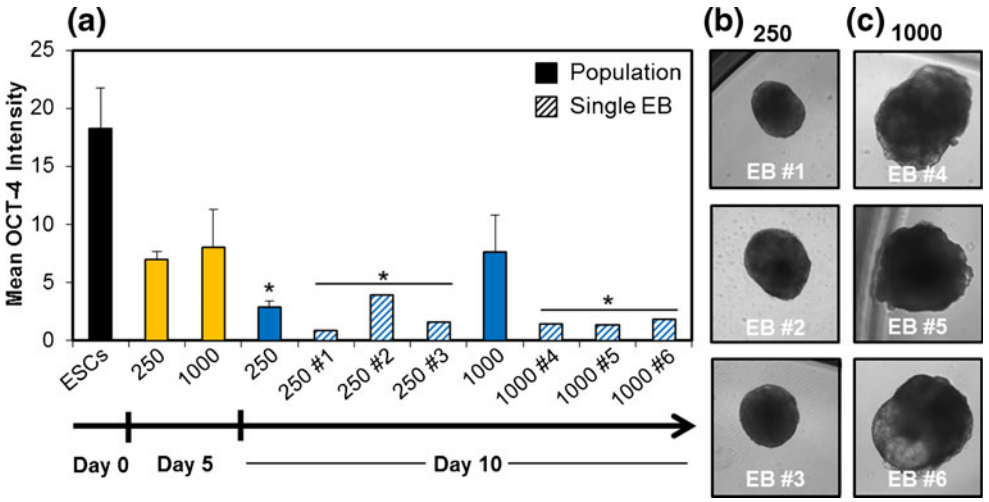

Fig. 6 Population and single EB OCT-4 expression. The mean intensity obtained from the cell trap device was assessed for each condition, including the single EBs (**a**). The single EBs of both sizes were imaged (**b**, **c**) immediately prior to their dissociation and loading at day 10 of differentiation. In general, single EBs exhibited lower OCT-4 expression than the population-averaged values (**a**), though the differences were not statistically significant ($p = 0.939$ for 250 cell EBs; $p = 0.137$ for 1,000 cell EBs). * indicates significant decrease in OCT-4 intensity compared to the day 0 starting population ($p < 0.05$)

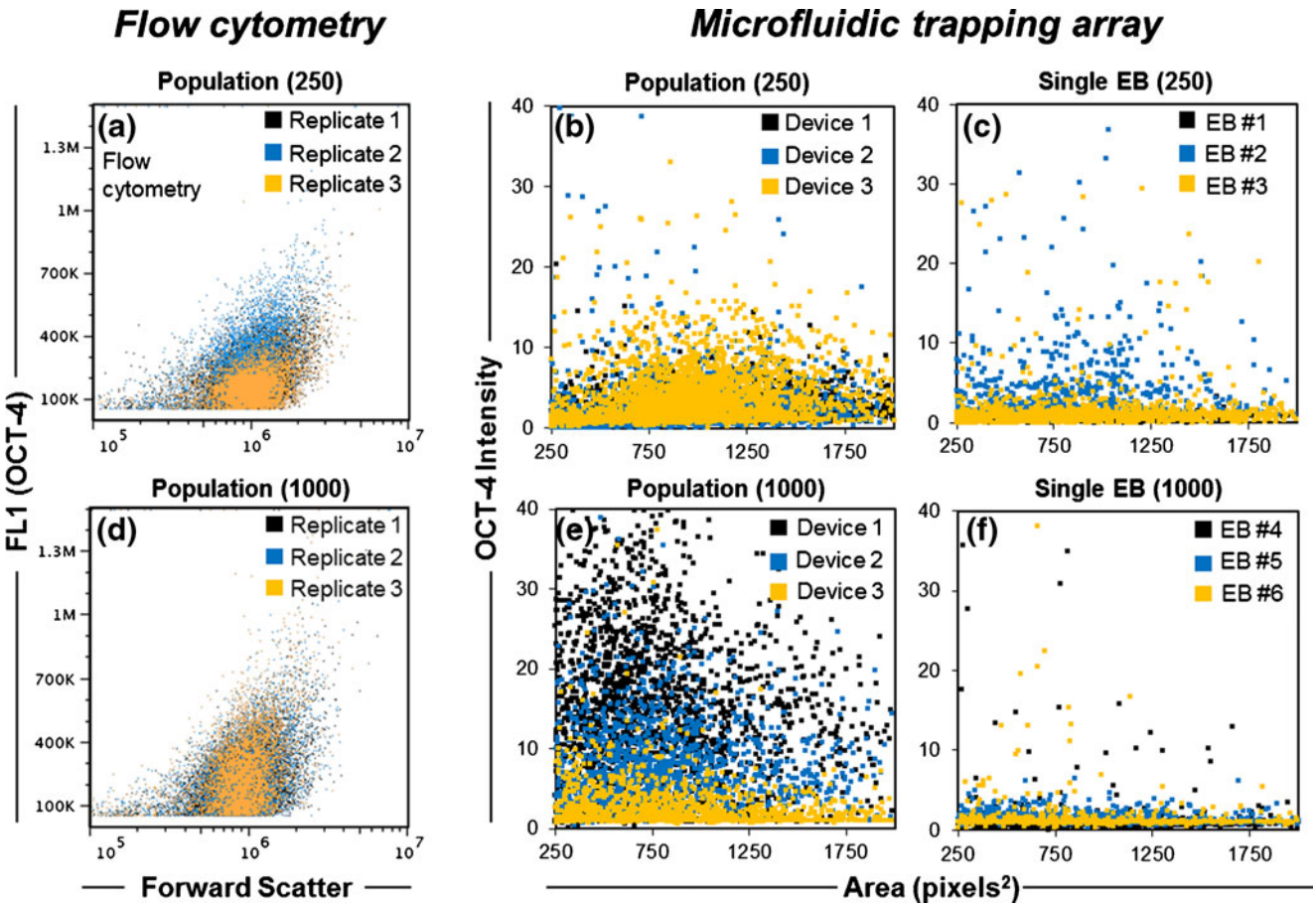

Fig. 7 Heterogeneity of OCT-4 expression in EB populations versus single EBs. Values of OCT-4 intensity vs. forward scatter (or cell size) were graphed as scatter plots for both population and single EB analysis of both sizes at day 10. Corresponding flow cytometry scatter plots for 250 cell EBs (**a**) and 1,000 cell EBs (**d**) are displayed for comparison. Similar shapes are observed between the 250 cell population (**b**) and single EBs (**c**) but differential patterns are observed in the 1,000 cell population (**e**) and single EBs (**f**)

toward many lineages, including cardiac (Maltsev et al. 1993; Xu et al. 2002), hematopoietic (Doetschman et al. 1985; Ng et al. 2005), and neural (Schuldiner et al. 2001; Wichterle et al. 2002). However, differentiation via EB methods typically gives rise to heterogeneity in the cell population, as most cells differentiate in parallel toward multiple lineages while some may remain undifferentiated. In addition to different media compositions, physical parameters, such as the size of the EBs, can contribute to phenotypic variation through the establishment of nutrient and oxygen gradients (Van Winkle et al. 2012). Therefore, the objective of this work was to examine EB heterogeneity on the single-cell level, which was accomplished using a microfluidic cell trap device in combination with on-chip staining and imaging. Information regarding the degree and heterogeneity of single cell OCT-4 expression was obtained for both a population of EBs and for single EBs. The results from the cell trap device were compared with flow cytometry and whole mount immunostaining to compare the overall OCT-4 expression as well as the heterogeneity of expression observed with each approach. Overall, assessing the variability of OCT-4 expression in single EBs in comparison with the variability in a population of EBs represents a novel approach for evaluating how heterogeneity is manifested in EB cultures.

Microfluidic systems are being increasingly used as instruments for sorting stem cells (Singh et al. 2013; Wu et al. 2010; Lillehoj et al. 2010) and for deciphering stem cell function owing to their capacity to array cells in a high-throughput fashion, to precisely deliver solutions in well-controlled spatial and temporal manner, and to enable real-time imaging. Several studies have examined microfluidic methods to control EB culture and differentiation on-chip (Fung et al. 2009; Khoury et al. 2010), although the devices previously developed do not include any downstream analysis of the single cells within the aggregates. Other studies have described devices which enable trapping of single-cell populations (Cui et al. 2011; Kumano et al. 2012; Lawrenz et al. 2012) for cell pairing and real-time monitoring, some of which have examined stem cell populations. Studies with hematopoietic

stem cells (HSCs) have been most often described, likely due to their non-adherent phenotype, and include investigations into the differences in proliferation and survival of normal (Lecault et al. 2011) and diseased HSCs (Faley et al. 2009), as well as the percentage of HSCs in different stages of the cell cycle (Kobel et al. 2012). Other microfluidic platforms capable of performing on-chip staining and imaging similar to flow cytometry have been described for a number of cell types as a means to decrease reagent volumes and the required cell sample size (Buhlmann et al. 2003; Wu et al. 2012), similar to advantages achieved with the device described in this paper. However, there has been a deficiency of microfluidic approaches describing the analysis of small tissue constructs, like EBs, that are difficult to evaluate using typical analytical tools owing to the high cell density and small cell numbers of individual aggregates. The ability to quantitatively examine the protein expression of the single cells that comprise individual EBs, as achieved with the hydrodynamic cell trap in this paper, could provide new information while also complementing emerging strategies offered by microfluidic-based single cell PCR systems (White et al. 2011; Zhong et al. 2008; Glotzbach et al. 2011) as a means to examine differential gene and protein expression patterns.

In order to substantiate the results obtained with the microfluidic cell trap, the outcomes were compared to those obtained via flow cytometry and whole mount immunostaining. Flow cytometry is perhaps the most common tool for examining single cell phenotype, and the results from the cell trap generally agreed with those obtained with flow cytometry (Fig. 3). However, some differences were observed for certain groups and time periods (i.e. Fig. 3, 250 cell EBs at day 10). Some divergence is to be expected due to the number of cells being sampled in each case. For flow cytometry, a minimum of 10,000 events were collected, and the contribution of non-specific binding could be removed with gates using an isotype control. In contrast, only approximately 2,000 cells were examined per microfluidic device. The fact that 20 % fewer cells were used for the cell traps compared to flow cytometry may account for some of the variability seen, although it is interesting to note that both analytical tools assessed only a fraction of the cells (< 0.5 %) present in an experimental replicate (approximately 2 million cells total). The other method used to compare the results of the cell trap was immunostaining and whole mount imaging using confocal microscopy (Fig. 5). While confocal microscopy is relatively low-throughput, it is useful in that it provides spatial information; however, the technique is technically limited due to poor optical penetration into embryoid bodies greater than 50 μm in diameter. Nevertheless, EBs imaged by confocal microscopy exhibited OCT-4 expression patterns that were consistent with the quantitative data obtained from the cell traps. For example, areas of bright and dim OCT-4 expression were observed in the 1,000 cell EBs at day 10 (Fig. 5d), which corresponded to the cell trap images (Fig. 2o) and histograms demonstrating the relative proportion of OCT-4 intensities of individual cells (Fig. 4f).

While flow cytometry can be used to evaluate the phenotypic state of a population of EB-derived cells, there is no current method that can easily be used to quantify the phenotypic diversity of single EBs because of the small numbers of cells in single EBs. Therefore, flow cytometry is unable to aid in the confirmation and deciphering of the lower OCT-4 expression detected in single EBs compared to the average population values (Fig. 6a). One caveat is that the fraction of the sampled population is very small (<1 % of the EBs from a plate of 1,500); therefore any observed differences may be based on the limited sampling due to the low throughput nature of the current method. When the variability in OCT-4 expression was inspected for the population and single EBs (Fig. 7), similar patterns were observed in the 250 cell EB population and single EBs, indicating that the individual EBs sampled were representative of the population and/or that variability between EBs (inter-EB variability) was less significant for the 250 cell aggregates and the variance of phenotypes within a single EB (intra-EB variability) governed heterogeneity. In contrast, the divergent patterns of OCT-4 expression observed between the population of 1,000 cell EBs and single EBs may indicate that the single EBs examined were not characteristic of the population, or it may signify that the variance of cell phenotypes between individual EBs (inter-EB variability) is greater for larger sized EBs.

The implications of greater inter-EB variability than intra-EB heterogeneity may be that that a culture process is impacting different aggregates in a divergent manner, which may indicate that some EBs are experiencing appreciably different environmental influences than others. On the other hand, if high intra-EB variability is present, this may imply that internal nutrient/oxygen gradients or contrasting local cell-cell interactions are the primary contributor(s) to the observed heterogeneity of cell phenotypes (Sachlos and Auguste 2008; Van Winkle et al. 2012). In general, the subtle differences observed in OCT-4 expression between different EB sizes are consistent with previous literature which has demonstrated that larger 1,000 cell EBs tend to exhibit a delayed temporal decrease of OCT-4 expression compared to smaller 250 cell EBs (White et al. 2013), as was found with all of the methods of analysis used in this study (Figs. 2, 4 and 5).

Overall, the development and subsequent validation of an approach to quantitatively assess information about individual EBs at a single cell resolution was established, leading to notable findings regarding the variance of OCT-4 expression within single EBs. In the future, coupling of single-cell analysis with long-term live cell imaging could provide additional information regarding the dynamics of protein expression and could lead to an improved understanding

about the underlying cause of heterogeneity in stem cell populations. Nevertheless, the approach described will be beneficial in evaluating the variability encountered during stem cell differentiation and can provide more specific information regarding single stem cell fate within complex multicellular aggregates.

Acknowledgments This work was supported by funding from the NIH R01EB010061(T.C.M.) and NIH R21EB012803 (H.L.), ARRA subaward under RC1CA144825 (H.L.), a Sloan Foundation Fellowship (H.L.), NSF CBET 0954578 (H.L.). J.L.W. is currently supported by a GAANN Fellowship (Department of Education P200A090099) and previously by an NSF IGERT (DGE 0965945).

References

F. Antonica, D.F. Kasprzyk, R. Opitz, M. Iacovino, X.-H. Liao, A.M. Dumitrescu, S. Refetoff, K. Peremans, M. Manto, M. Kyba, S. Costagliola, Nature **491**, 66 (2012)

C.L. Bauwens, R. Peerani, S. Niebruegge, K.A. Woodhouse, E. Kumacheva, M. Husain, P.W. Zandstra, Stem Cells **26**, 2300 (2008)

A.M. Bratt-Leal, R.L. Carpenedo, T.C. McDevitt, Biotechnol. Prog. **25**, 43 (2009)

C. Buhlmann, T. Preckel, S. Chan, G. Luedke, M. Valer, J. Biomol. Tech. **14**, 119 (2003)

D.G. Buschke, D.J. Hei, K.W. Eliceiri, B.M. Ogle, in *Stem Cell-Based Tissue Repair*, ed. by R. Gorodetsky (Royal Society of Chemistry, London, 2010), pp. 55–140

R.L. Carpenedo, C.Y. Sargent, T.C. McDevitt, Stem Cells **25**, 2224 (2007)

C. Chazaud, Y. Yamanaka, T. Pawson, J. Rossant, Dev. Cell **10**, 615 (2006)

Y.Y. Choi, B.G. Chung, D.H. Lee, A. Khademhosseini, J.-H. Kim, S.-H. Lee, Biomaterials **31**, 4296 (2010)

K. Chung, C.A. Rivet, M.L. Kemp, H. Lu, Anal. Chem. **83**, 7044 (2011)

K. Chung, J. Wallace, S.-Y. Kim, S. Kalyanasundaram, A.S. Andalman, T.J. Davidson, J.J. Mirzabekov, K.A. Zalocusky, J. Mattis, A.K. Denisin, S. Pak, H. Bernstein, C. Ramakrishnan, L. Grosenick, V.Gradinaru, K. Deisseroth, Nature **497**, 332 (2013)

S. Cui, Y. Liu, W. Wang, Y. Sun, Y. Fan, Biomicrofluidics **5**, 32003 (2011)

T.C. Doetschman, H. Eistetter, M. Katz, W. Schmidt, R. Kemler, J. Embryol. Exp. Morphol. **87**, 27 (1985)

M. Eiraku, N. Takata, H. Ishibashi, M. Kawada, E. Sakakura, S. Okuda, K. Sekiguchi, T. Adachi, Y. Sasai, Nature **472**, 51 (2011)

T. Enver, S. Soneji, C. Joshi, J. Brown, F. Iborra, T. Orntoft, T. Thykjaer, E. Maltby, K. Smith, R.A. Dawud, M. Jones, M. Matin, P. Gokhale, J. Draper, P.W. Andrews, Hum. Mol. Genet. **14**, 3129 (2005)

T. Enver, M. Pera, C. Peterson, P.W. Andrews, Cell Stem Cell **4**, 387 (2009)

M. Esner, J. Pachernik, A. Hampl, P. Dvorak, Int. J. Dev. Biol. **46**, 817 (2002)

S.L. Faley, M. Copland, D. Wlodkowic, W. Kolch, K.T. Seale, J.P. Wikswo, J.M. Cooper, Lab Chip **9**, 2659 (2009)

W.-T. Fung, A. Beyzavi, P. Abgrall, N.-T. Nguyen, H.-Y. Li, Lab Chip **9**, 2591 (2009)

J.P. Glotzbach, M. Januszyk, I.N. Vial, V.W. Wong, A. Gelbard, T. Kalisky, H. Thangarajah, M.T. Longaker, S.R. Quake, G. Chu, G.C. Gurtner, PloS One **6**, e21211 (2011)

T. Graf, M. Stadtfeld, Cell Stem Cell **3**, 480 (2008)

K. Hayashi, S.M.C.D.S. Lopes, F. Tang, M.A. Surani, Cell Stem Cell **3**, 391 (2008)

S.-H. Hong, T. Werbowetski-Ogilvie, V. Ramos-Mejia, J.B. Lee, M. Bhatia, Stem Cell Res. **5**, 120 (2010)

S.R. Hough, A.L. Laslett, S.B. Grimmond, G. Kolle, M.F. Pera, PLoS One **4**, e7708 (2009)

Y.-S. Hwang, B.G. Chung, D. Ortmann, N. Hattori, H.-C. Moeller, A. Khademhosseini, Proc. Natl. Acad. Sci. **106**, 16978 (2009)

J.P. Jung, J.M. Squirrell, G.E. Lyons, K.W. Eliceiri, B.M. Ogle, Trends Biotechnol. **30**, 233 (2012)

S.J. Kattman, T.L. Huber, G.M. Keller, Dev. Cell **11**, 723 (2006)

G. Keller, Genes Dev. **19**, 1129 (2005)

M. Khoury, A. Bransky, N. Korin, L.C. Konak, G. Enikolopov, I. Tzchori, S. Levenberg, Biomed. Microdevices **12**, 1001 (2010)

M.A. Kinney, R. Saeed, T.C. McDevitt, Integr. Biol. **4**, 641 (2012)

S.A. Kobel, O. Burri, A. Griffa, M. Girotra, A. Seitz, M.P. Lutolf, Lab Chip **12**, 2843 (2012)

I. Kumano, K. Hosoda, H. Suzuki, K. Hirata, T. Yomo, Lab Chip **12**, 3451 (2012)

H. Kurosawa, J. Biosci. Bioeng. **103**, 389 (2007)

A. Lawrenz, F. Nason, J.J. Cooper-White, Biomicrofluidics **6**, 2411201 (2012)

A. Leahy, J.-W. Xiong, F. Kuhnert, H. Stuhlmann, J. Exp. Zool. **284**, 67 (1999)

V. Lecault, M. Vaninsberghe, S. Sekulovic, D.J.H.F. Knapp, S. Wohrer, W. Bowden, F. Viel, T. McLaughlin, A. Jarandehei, M. Miller, D. Falconnet, A.K. White, D.G. Kent, M.R. Copley, F. Taghipour, C.J. Eaves, R.K. Humphries, J.M. Piret, C.L. Hansen, Nat. Methods **8**, 581 (2011)

P.B. Lillehoj, H. Tsutsui, B. Valamehr, H. Wu, C.-M. Ho, Lab Chip **10**, 1678 (2010)

V.A. Maltsev, J. Rohwedel, J. Hescheler, A.M. Wobus, Mech. Dev. **44**, 41 (1993)

J.M. Messana, N.S. Hwang, J. Coburn, J.H. Elisseeff, Z. Zhang, J. Tissue Eng. Regen. Med. **2**, 499 (2008)

J.C. Mohr, J. Zhang, S.M. Azarin, A.G. Soerens, J.J. de Pablo, J.A. Thomson, G.E. Lyons, S.P. Palecek, T.J. Kamp, Biomaterials **31**, 1885 (2010)

R. Nair, A.V Ngangan, M.L. Kemp, T.C. McDevitt, PLoS One **7**, e42580 (2012)

E.S. Ng, R.P. Davis, L. Azzola, E.G. Stanley, A.G. Elefanty, Blood **106**, 1601 (2005)

S. Niebruegge, C.L. Bauwens, R. Peerani, N. Thavandiran, S. Masse, E. Sevaptisidis, K. Nanthakumar, K. Woodhouse, M. Husain, E. Kumacheva, P.W. Zandstra, Biotechnol. Bioeng. **102**, 493 (2009)

W. Risau, H. Sariola, H.G. Zerwes, J. Sasse, P. Ekblom, R. Kemler, T. Doetschman, Development (Cambridge, England) **102**, 471 (1988)

E. Sachlos, D.T. Auguste, Biomaterials **29**, 4471 (2008)

A.A. Sajini, L.V. Greder, J.R. Dutton, J.M.W. Slack, Dev. Biol. **371**, 170 (2012)

T. Schroeder, Nat. Methods **8**, S30 (2011)

M. Schuldiner, R. Eiges, A. Eden, O. Yanuka, J. Itskovitz-Eldor, R.S. Goldstein, N. Benvenisty, Brain Res. **913**, 201 (2001)

J. Silva, A. Smith, Cell **132**, 532 (2008)

A. Singh, S. Suri, T. Lee, J.M. Chilton, M.T. Cooke, W. Chen, J. Fu, S.L. Stice, H. Lu, T.C. McDevitt, A.J. García, Nat. Methods **10**, 438 (2013)

H. Suga, T. Kadoshima, M. Minaguchi, M. Ohgushi, M. Soen, T. Nakano, N. Takata, T. Wataya, K. Muguruma, H. Miyoshi, S. Yonemura, Y. Oiso, Y. Sasai, Nature **480**, 57 (2011)

Y. Toyooka, D. Shimosato, K. Murakami, K. Takahashi, H. Niwa, Development **135**, 909 (2008)

M.D. Ungrin, C. Joshi, A. Nica, C. Bauwens, P.W. Zandstra, PloS One **3**, e1565 (2008)

B. Valamehr, S.J. Jonas, J. Polleux, R. Qiao, S. Guo, E.H. Gschweng, B. Stiles, K. Kam, T.M. Luo, O.N. Witte, X. Liu, B. Dunn, H. Wu, Proc. Natl. Acad. Sci. **105**, 14459 (2008)

A.P. Van Winkle, I.D. Gates, M.S. Kallos, Cells Tissues Organs **196**, 34 (2012)
A.K. White, M. VanInsberghe, O.I. Petriv, M. Hamidi, D. Sikorski, M. a Marra, J. Piret, S. Aparicio, and C. L. Hansen. Proc. Natl. Acad. Sci. **108**, 13999 (2011)
D.E. White, M.A. Kinney, T.C. McDevitt, M.L. Kemp, PLoS Comput. Biol. **9**, e1002952 (2013)
H.Wichterle, I. Lieberam, A. Jeffery, T.M. Jessell, Cell **110**, 385 (2002)
H.-W. Wu, R.-C. Hsu, C.-C. Lin, S.-M. Hwang, G.-B. Lee, Biomicrofluidics **4**, 024112 (2010)
M. Wu, T.D. Perroud, N. Srivastava, C.S. Branda, K.L. Sale, B.D. Carson, K.D. Patel, S.S. Branda, A.K. Singh, Lab Chip **12**, 2823 (2012)
C. Xu, S. Police, N. Rao, M.K. Carpenter, Circ. Res. **91**, 501 (2002)
J.F. Zhong, Y. Chen, J.S. Marcus, A. Scherer, S.R. Quake, C.R. Taylor, L.P. Weiner, Lab Chip **8**, 68 (2008)